Commun Nonlinear Sci Numer Simulat 44 (2017) 159–166

Contents lists available at ScienceDirect

Commun Nonlinear Sci Numer Simulat

journal homepage: www.elsevier.com/locate/cnsns

Research paper

Wavepacket delocalization, self-trapping and fragmentation in discrete chains with relaxing nonlinearity

R.P.A. Lima[a,b], Iram Gléria[a], C.H. Cícero[a], M.L. Lyra[a,*], F.A.B.F. de Moura[a]

[a] GFTC Instituto de Física, Universidade Federal de Alagoas, Maceió AL 57072-970, Brazil
[b] GISC Instituto de Física, Universidade Federal de Alagoas, Maceió AL 57072-970, Brazil

ARTICLE INFO

Article history:
Received 11 January 2016
Revised 22 July 2016
Accepted 8 August 2016
Available online 9 August 2016

Keywords:
Localization
Third-order nonlinearity
Wavepacket dynamics
Self-trapping transition

ABSTRACT

The discrete nonlinear Schrodinger equation (DNSE) describes wave phenomena in several physical contexts, ranging from electronic transport in crystalline chains to light propagation in nonlinear media and Bose-Einstein condensates. Here, we study the influence of the nonlinear response time on the temporal evolution of a wavepacket initially localized in a single site of a finite closed chain. Distinct long-time wavepacket distributions are identified as a function of the nonlinear strength χ and the characteristic relaxation time τ. Besides the more standard delocalized and self-trapped regimes, we report the occurrence of intermediate phases. In one of them the wavepacket self-focus in the opposite chain site. A phase with asymptotically fragmented wavepackets also develops. A crossover regime on which the ultimate wavepacket distribution is strongly dependent on the precise set of model parameters is also identified. We provide the full phase diagram related to the long-time wavepacket distribution in the (χ, τ) space.

1. Introduction

Studies of the dynamics of quantum wavepackets have impelled a deeper understanding of several relevant condensed matter physics aspects [1–3]. In the context of transport properties, the presence of nonlinear contributions promotes the emergence of new phenomenologies. For example, the dynamics of Bose–Einstein Condensates (BEC) is well described by the Gross–Pitaevskii (GP) nonlinear equation [4–7]. The (GP) nonlinear equation was originally derived by assuming that only binary collisions are relevant in the low-energy regime. The parameter that characterizes these collisions, called the s-wave scattering length, is usually much smaller than the average distance between atoms. Numerical and analytical treatments of the (GP) nonlinear equation provide a detailed description of the ground "BEC" state ($T = 0$) as well as low-temperature effects.

In the framework of electronic transport, the effective contribution of the interaction between electrons and optical phonons is well described by a nonlinear Schrodinger equation [8,9]. The nonlinearity arising from the electron-phonon interaction has a character similar to the nonlinear local potential in the (GP) nonlinear equation: it appears as a local potential proportional to the square modulus of the wavepacket. One of the most interesting phenomenon within the electronic context is the self trapping (ST) which occurs when the nonlinearity strength exceeds a critical value the order of the energy bandwidth [9–17]. When ST takes place, an initially localized wavepacket does not spread over the system,

* Corresponding author. Fax: +55 82 3214 1645.
E-mail addresses: rodrigo@fis.ufal.br (R.P.A. Lima), iram@fis.ufal.br (I. Gléria), marcelo@fis.ufal.br (M.L. Lyra), fidelis@fis.ufal.br (F.A.B.F. de Moura).

http://dx.doi.org/10.1016/j.cnsns.2016.08.002
1007-5704/

remaining localized around its initial position. The effect of nonlinearity and the dependence of the ST phenomenon on the intrinsic lattice geometry have attracted a great interest in the last years. For example, a detailed study of the ST transition in square and honeycomb lattices was reported in ref. [17]. It was shown that the ST threshold continuously grow as a function of the initial wavepacket width. The effect of nonlinear diagonal potential was studied in DNA-like segments [18]. Self-trapping at large nonlinearity was also reported in carbon nanotubes with strong electron-phonon coupling [19]. In ref. [20] the influence of electron-lattice interaction on the stability of uniform electronic wavepackets on chains and fullerenes was also considered.

The electronic transport in discrete lattices with non-adiabatic nonlinearity was the subject of several recent studies. In ref. [11] the problem of electronic ST in chains with a non-adiabatic delayed electron-phonon coupling was investigated. It was shown that for a delayed nonlinearity below the electronic bandwidth, ST transition may still occur. It was also demonstrated that for slowly responding media, ST only takes place for very strong nonlinearity. By considering a one-dimensional chain, the slow relaxation of the nonlinearity was show to be responsible for the absence of a delocalized regime and the emergence of a complex wavepacket self-focusing regime [21]. Ref. [13] dealt with the competition between disorder and a finite nonlinear response time. It was numerically demonstrated that no sub-diffusive spreading of the second moment of the wavepacket distribution takes place when the finite response time of the nonlinearity is taken into account, contrasting with the sub-diffusive spreading in instantaneously responding media [22]. Such re-localization was latter explained as resulting from the energy drift towards the band edge [23]. Recently, studies in C_{60} buckyballs provided evidence that the relaxation process of the nonlinearity has a profound impact in the wavepacket dynamics and in the formation of ST stationary states [24]. Moreover, the one-electron wavepacket dynamics in a C_{60} buckyball topology with a relaxing nonlinearity was studied in ref. [25]. By considering distinct initial conditions, the delocalization/self-trapping transition as a function of the nonlinear strength and relaxation time was characterized. It was shown that the phase-diagram exhibits a complex pattern signaling a re-entrant behavior of the transition which is strongly sensitive to the initial wavepacket distribution.

In this work, we provide a detailed study of the dynamics of initially localized wavepackets governed by a discrete nonlinear one-dimensional Schrodinger equation on which the nonlinearity exhibits a relaxation process. We will follow the temporal evolution of the wavepacket and characterize its spacial extension and location by computing the participation number, the return probability and the opposite site occupation probability. The delocalization/self-trapping transition will be characterized as a function of the nonlinear strength and the typical relaxation time. We compile our main results in a phase-diagram, identifying up to five parameter set regions on which the wavepacket displays quite distinct dynamic evolutions.

2. Model and formalism

We will consider the time-evolution of a one-dimensional wavepacket under the action of a non-instantaneous third-order nonlinearity. By considering a Debye-like relaxation of the nonlinear contribution [21,24], the dynamics can be studied using the following pair of coupled equations:

$$\begin{aligned} i\dot{\phi}_j &= \phi_{j+1} + \phi_{j-1} + A_j\phi_j \\ \dot{A}_j &= -\frac{1}{\tau}(A_j + \chi|\phi_j|^2), \end{aligned} \tag{1}$$

where the wavepacket is represented in the localized orbitals Wannier representation by $|\Psi\rangle = \sum_j \phi_j(t)|j\rangle$. The term A_j is the nonlinear time-dependent contribution to the effective on site potential, whose relaxation has a characteristic time τ. The strength of the nonlinear contribution is parametrized by χ. In the context of electronic transport, it raises from the strong coupling with optical phonons. We consider the initial wavepacket fully localized at the center of chain (represented by $N/2$), *i.e* $\phi_j(t=0) = \delta_{j,N/2}$, and use periodic boundary conditions. To probe the wavepacket dynamics, we follow the time-evolution of the participation number $\xi(t)$ defined as [21,26]

$$\xi(t) = \left[\sum_j |\phi_j|^4\right]^{-1}. \tag{2}$$

Usually the participation number is a good estimate of the number of sites that effectively contribute to wavepacket distribution. For uniformly extended states, $\xi(t)$ equals the total number of sites N. For strongly localized states, the participation number $\xi(t) \ll N$, being of the order of the localization length. In addition, we compute the return probability defined as [21]:

$$R(t) = |\phi_{N/2}(t)|^2. \tag{3}$$

The wavepacket escapes from its initial position when the amplitude $\phi_{N/2}(t)$, and consequently the return probability, decreases as t increases. Conversely, the amplitude remains finite for a wavepacket localized around its initial position. We also compute the occupancy probability of the opposite site $O(t)$, calculated at the (N)th site and given by [21]:

$$O(t) = |\phi_N(t)|^2. \tag{4}$$

This quantity characterizes some particular cases on which the wavepacket focuses in the opposite side of the chain after spreading over the lattice.

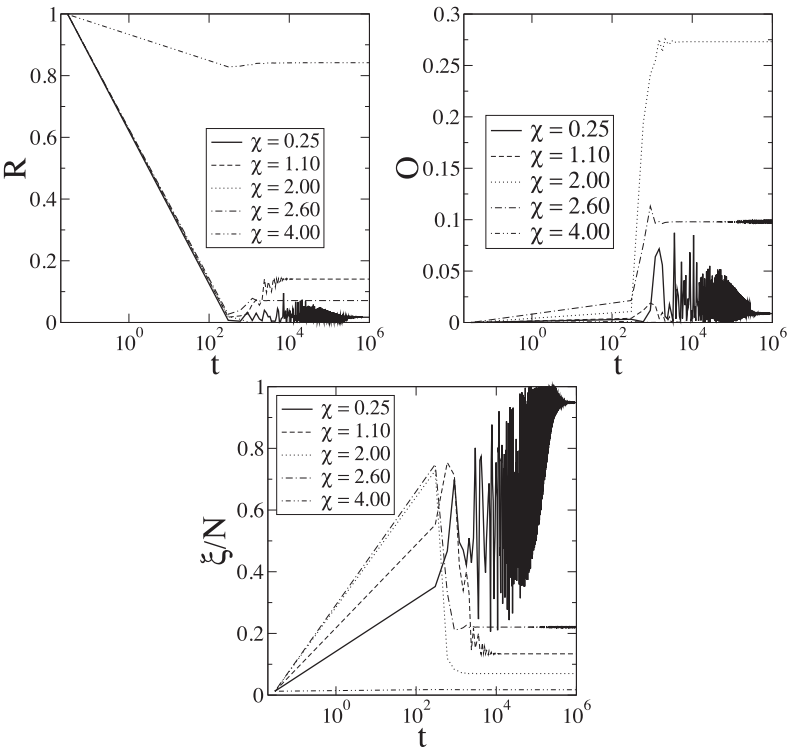

Fig. 1. Return probability $R(t)$, opposite site probability $O(t)$ and the scaled participation number ξ/N versus time for $\tau = 1$ and several values of nonlinearity χ.

3. Results and discussions

We present results from the numerical solution of Eq. 1, obtained by employing an eight-th order Runge–Kutta algorithm [27]. The wavefunction norm ($N(t) = \sum_j |\phi_j|^2$) was accompanied with an accuracy of $|1 - N(t)| < 10^{-8}$. As pointed out before, a fully localized initial wavepacket $\phi_j(t = 0) = \delta_{j,N/2}$ and periodic boundary conditions were considered. Calculations were done considering a closed chain with $N = 80$ sites. In Fig. 1 we collect our results for the return probability $R(t)$, the opposite probability $O(t)$ and the scaled participation number ξ/N versus time for $\tau = 1$ and several values of nonlinearity χ. We observe a series of specific features in each one of these quantities. All of them exhibit a strong dependence with the nonlinearity strength χ. The combined analysis of these three quantities provides precise information on the nature of the asymptotic wavepacket. For example, for $\xi = 0.25$ we observe that both $R(t)$ and $O(t)$ goes to zero as time increases (actually they become of the order of $1/N$). It suggests that the wavepacket is not located around the site $N/2$ nor the site N. Moreover, by analyzing the increasing of the participation number for $\chi = 0.25$, we conclude that the wavepacket is extended all over the chain.

An interesting intermediate dynamics is illustrated for the particular case of $\chi = 2$. We observe that the return probability goes to zero as time increases. By analyzing just the data of $R(t)$, one may erroneously conclude that the state became extended. However, when analyzing the scaled participation number we see that for long times, only a finite fraction of the chain is covered by the wavepacket. The final conclusion about the nature of the wavepacket can be found by looking at the opposite site probability. We see that for $\chi = 2$, $O(t)$ is quite close to unity suggesting the wavepacket becomes localized around the opposite position N. For $\chi = 2.60$ we observe that both the opposite site probability and the return probabilities remain finite, while the asymptotic participation number is small. This behavior points to a fragmentation of the wavepacket. Finally, for large values of the nonlinearity strength ($\chi = 4.0$), the return probability is large, signaling the wavepacket self-trapping.

By using the procedure described previously, we can analyze in detail the nature of the wavepacket for each pair of parameters (τ, χ). We tune χ and τ respectively within the ranges [0, 5] and [0, 1] to provide the long-time value of the return probability $R_\infty = R(t \to 10^6)$, opposite site probability $O_\infty = O(t \to 10^6)$ and the scaled participation number $\tilde{\xi}_\infty = \xi(t \to 10^6)/N$. In Figs. 2–4, we plot the long-time behavior of these quantities within the (τ, χ) parameter space. We observe in Fig. 2 that, for strong nonlinearity values ($\chi > 4$), the return probability is close to unity regardless of τ. This suggest a localized state. In Figs. 3 and 4 we see that the opposite probability and the scaled participation number vanishes for ($\chi > 4$). Therefore, the region with strong nonlinearity seems to ban the wavepacket diffusion. This is in good agreement with previous works that pointed out the wavepacket self-trapping when the nonlinearity is larger than the quantum band-

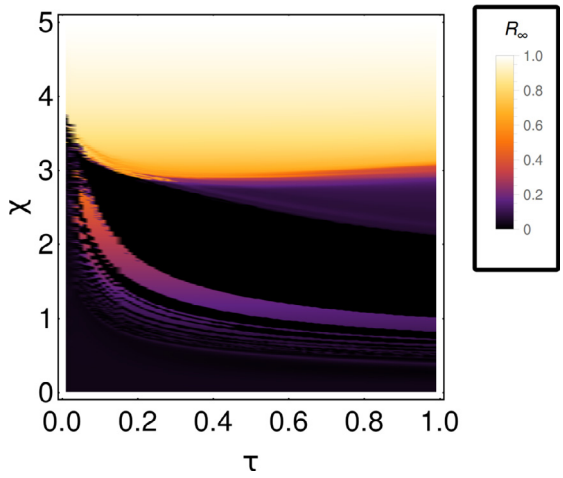

Fig. 2. Density plot of the long-time value of the return probability $R_\infty = R(t \to 10^6)$ in the $(\tau,\ \chi)$ parameter space.

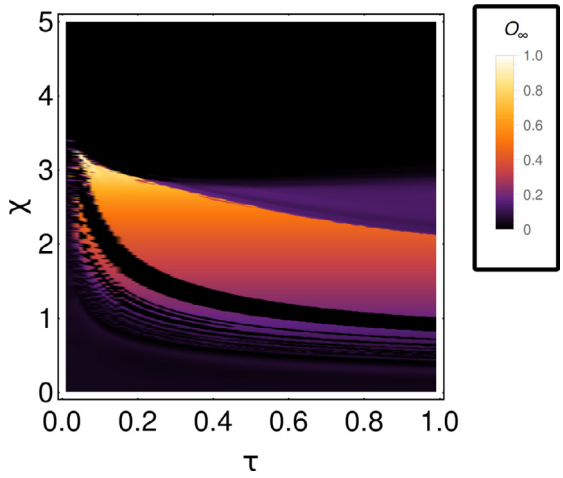

Fig. 3. The long-time behavior of the opposite site probability $O_\infty = O(t \to 10^6)$ in the $(\tau,\ \chi)$ parameter space.

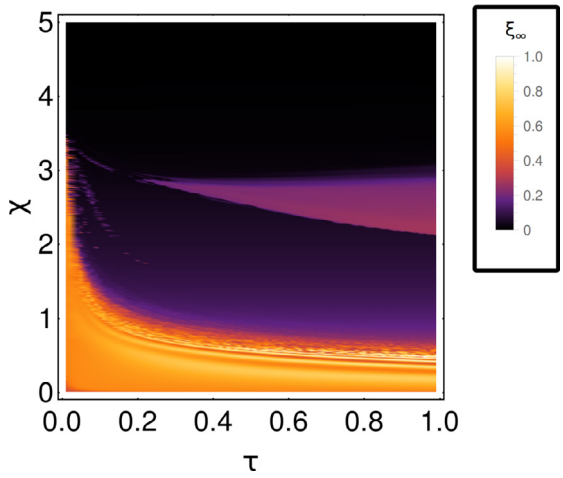

Fig. 4. The long-time behavior of the scaled participation number $\tilde{\xi}_\infty = \xi(t \to 10^6)/N$ in the $(\tau,\ \chi)$ parameter space.

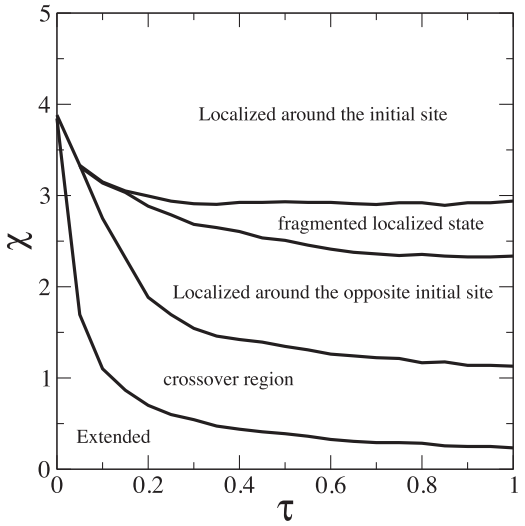

Fig. 5. Phase diagram in the χ, τ parameter space. Our calculations reveal the existence of four distinct phases: self trapping around the initial site, extended, localized around the opposite site and a fragmented localized state. In the crossover region, the wavepacket dynamics is strongly dependent on the specific parameters set.

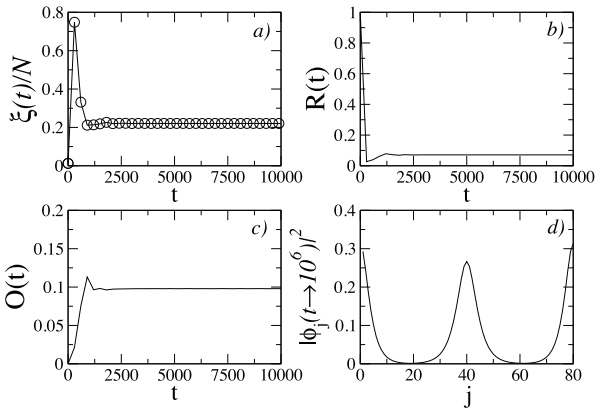

Fig. 6. (a–c) Participation number, the return and opposite site probabilities versus time for $\tau = 0.6$ and $\chi = 2.6$. (d) The wavepacket profile for long-times ($|\phi_j(t \to 10^6)|^2 \times j$) showing a fragmented localized distribution.

width. The extended behavior appears in the regime of weak nonlinear coupling. Notice that delocalization develops at a wider range of nonlinear couplings in the regime of fast nonlinear response (small τ).

For intermediate values of χ and τ, our calculations suggest the focusing of the wavepacket in the site opposite to the initial position. We see that both the return probability and the scaled participation number assume small values while the opposite site probability is close to unity. In Fig. 5, we present the phase diagram in the (χ, τ) parameter space. Four different phases and a "crossover region" can be identified. The phases we were able to characterize are: self-trapping around the initial site, extended, localized around the opposite site and a fragmented localized state. In the fragmented localized phase, the wavepacket initially spreads over most of the lattice sites and, after a long time lapse, it splits in nearly disjoint parts to focus around distinct chain sites. In some isolated cases the wavepacket focus a finite fraction around the initial position and a small fraction in the opposite site. Such phase is often characterized by a kind of "fragmented" localized state in the long-time limit. Fig. 6 illustrates this intermediate regime, where we plot $R(t)$, $O(t)$, $\xi(t)/N$ and the wavepacket profile for large t. The values $\tau = 0.6$ and $\chi = 2.6$ were chosen to exemplify the behavior of the "fragmented" localized phase. The participation number versus time shows an initial increase, almost up to the system size. Moreover, the return probability decreases nearly to zero while the opposite site probability increases. In summary, the wavepacket initially spreads throughout the chain. After this initial transient, the participation number decreases, while the return and opposite probabilities asymptote to finite values. These calculations suggest that, for large times, the wavepacket evolves towards a fragmented localized state. This can be seen in the plot of $|\phi_j(t \to 10^6)|^2 \times j$. These results thus unveil the existence of a counter-intuitive intermediate dynamics strongly related to the nonlinearity and its relaxation process. Initially there is a

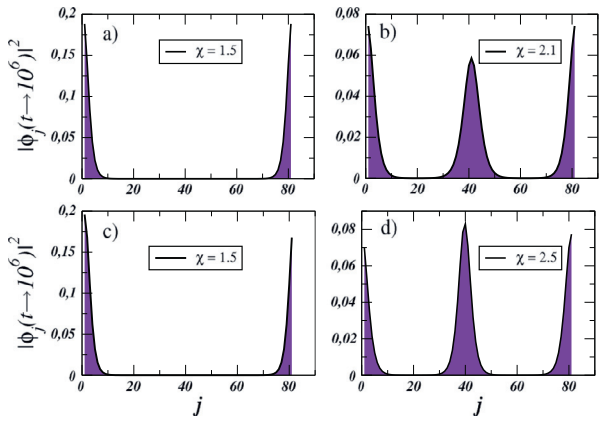

Fig. 7. Asymptotic (long-time) wavepacket distribution for some representative values of the nonlinear strength and chain size $N = 80$. The initial wavepacket has a Gaussian profile with (a and b) uniform and (c and d) random phases. Notice that the unusual fragmented and opposite localized states arise irrespective to the initial wavepacket distribution.

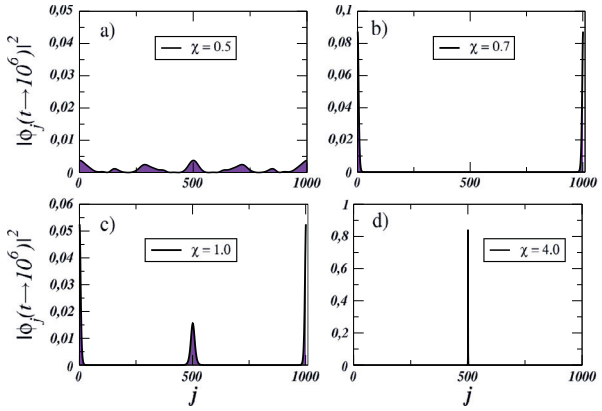

Fig. 8. Asymptotic (long-time) wavepacket distribution for some representative values of the nonlinear strength. The initial wavepacket was considered to be a fully localized state in the center of a closed chain with $N = 1000$ sites. (a) $\chi = 0.5$ leading to a delocalized chaotic-like state; (b) $\chi = 0.7$ corresponding to a asymptotic state localized around the opposite site; (c) $\chi = 1.0$ for which the states becomes fragmented around the initial and opposite sites; (d) $\chi = 4.0$ corresponding to a self-trapped state around the initial site.

macroscopic spread of the wavepacket followed by a self-focusing in distinct places of the chain, resulting in the wavepacket fragmentation.

The crossover region contains some similarities with the fragmented phase. For some specific values of τ and χ, the wavepacket remains almost completely localized in the opposite site and a finite small fraction in the initial site (e.g. $\tau \approx 0.5$ and $0.5 < \chi < 1.3$). For some other cases the situation follow the opposite trend: a mayor part of the wavepacket remains trapped around the initial site and a finite small fraction goes to the opposite site (e.g. $\tau \approx 0.1$ and $\chi \approx 3$). In this crossover region self-focusing develops after a long transient and the ultimate distribution of the wavepacket is strongly dependent on the specific parameter set, signaling a chaotic-like dynamics.

The above results indicate that, besides the usual delocalized and self-trapped states, the wavepacket can evolve to fragmented or opposite localized states. In order to verify that the emergence of these states is robust against the initial wavepacket distribution, we followed the wavepacket dynamics of Gaussian packets with uniform and random phases. Illustrative asymptotic profiles of the wavepacket are plotted in Fig. 7 for representative values of the nonlinear strength, showing that such unusual localized states are attractors of the dynamics in certain regions of the parameter space, irrespective to the actual form of the initial wavepacket. Further, we investigated that these localized states would also emerge when the wavepacket propagates in much longer chains. In Fig. 8, we plot asymptotic wavepacket profiles considering chains with $N = 1001$ sites. Here again, fragmented and opposite localized states are present. These results indicate that fragmented and opposite localized states, besides the usual self-trapped and delocalized states are attractors of the dynamics of the nonlinear Schrodinger equation with a relaxing nonlinearity.

In order to develop more physical insight on the mechanism leading to each asymptotic wavepacket state, we followed the temporal evolution of the wavepacket distribution for some representative cases. The results are depicted in Fig. 9 where we present density plots of the wavepacket. For a very weak nonlinearity, the initially localized state spreads having

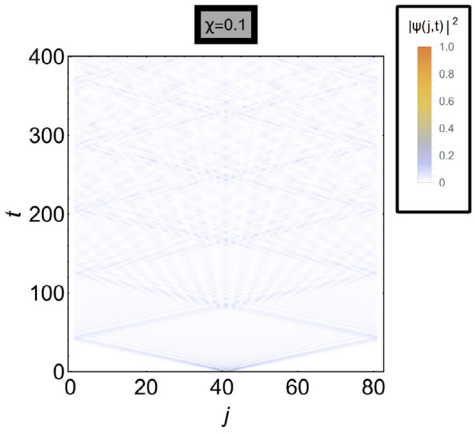

(a) $\chi = 0.1$ for which, after the initial transient, the wavepacket remains delocalized although presenting chaotic fluctuations;

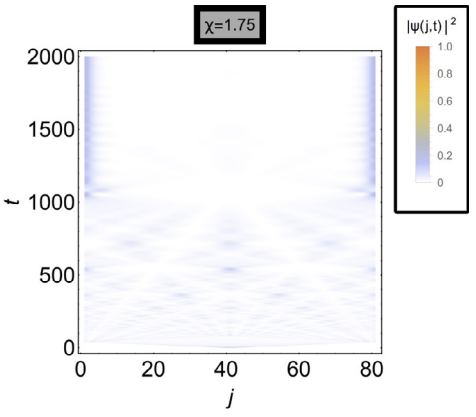

(b) $\chi = 1.75$ on which the delocalized state is unstable and a dynamic transition drives the system to a state localized around the opposite site;

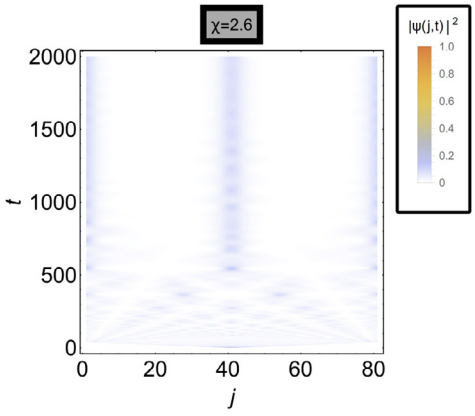

(c) $\chi = 2.6$ for which the state becomes a fragmented localized state after the dynamic transition;

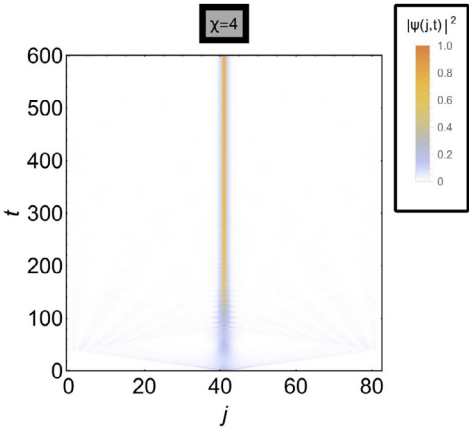

(d) $\chi = 4$ for which the state remains mainly trapped around the initial site.

Fig. 9. Density plots of the time-evolution of the wavepacket distribution for some representative values of the nonlinear coupling. The initial wavepacket was considered to be fully localized at the center of a closed chain with $N = 80$ sites.

wavefronts traveling to the left and right. After these fronts collision in the opposite site, they continuous to travel and progressively generate a delocalized chaotic-like state. Such delocalized state remains stable after very long run times. For larger nonlinear strengths, the chaotic delocalized state becomes unstable and a dynamic transition drives the wavepacket either towards the initial site, the opposite site (as shown in Fig. 9b), or to a fragmented state (Fig. 9c). We would like to stress that dynamic transitions have been previously reported to take place in nonlinear systems with a relaxing nonlinearity as, for example, in the time evolution of non-adiabatic nonlinear quantum dimers [28]. For stronger nonlinear strengths a finite fraction of the wavepacket remains trapped in the initial site, as shown in Fig. 9d.

4. Summary and conclusions

In summary, we studied the influence of the nonlinearity relaxation process on the wavepacket dynamics governed by a third-order discrete nonlinear Schrodinger equation. We focused our attention on the dynamics of an initial wavepacket fully localized in a single site of a finite linear chain with periodic boundary conditions. Distinct time evolutions of the wavepacket have been identified as a function of the nonlinear strength χ and its typical relaxation time τ. The standard self-trapped state predominates at strong nonlinearities at which the wavepacket remains trapped in a narrow segment

around its initial position. In the regime of weak nonlinearities, the wavepacket delocalizes and spreads all over the chain in the long time limit. We unveiled non-conventional intermediate regimes on which the wavepacket delocalizes during a short transient time before self-focusing. The ultimate focusing can be either around the initial position, around the opposite chain site, or even lead to the wavepacket fragmentation. Right above the boundary line in the (χ, τ) parameter space delimiting the phase with an asymptotically stable extended wavepacket, self-focusing develops after a very long transient time. This leads to a crossover regime on which the asymptotic wavepacket distribution is quite sensible to the precise set of model parameters, characteristic of a chaotic-like dynamics. It would be interesting to have future efforts aiming to investigate how the nonlinear response time affects the precise route between the lost of stability of the extended state, which is mainly driven by a modulational instability process [29], and the ultimate self-trapped state. The present results evidence that the relaxation process of the nonlinear response plays a relevant role in the wavepacket dynamics which has to be taken carefully into account when analyzing wave-like phenomena in nonlinear media.

Acknowledgments

This work was partially supported by CNPq, CAPES (PVE-A121), and FINEP (Federal Brazilian Agencies), as well as FAPEAL (Alagoas State Agency).

References

[1] Abrahams E, Anderson PW, Licciardello DC, Ramakrishnan TV. Phys Rev Lett 1979;42:673.
[2] Kramer B, MacKinnon A. Rep Prog Phys 1993;56:1469; Ziman TAL. Phys Rev Lett 1982;49:337 For a review see, e.g.; Lifshitz IM, Gredeskul SA, Pastur LA. Introduction to the Theory of Disordered Systems 1988 (Wiley, New York, 1988).
[3] Abrahams E, Anderson PW, Licciardello DC, Ramakrishnan TV. Phys Rev Lett 1979;42:673.
[4] Dalfovo F, Giorgini S, Pitaevskii LP, Stringari S. Rev Mod Phys 1999;71:463.
[5] Pitaevskii LP. Zh Eksp Teor Fiz 1961;40:646. [Sov. Phys. JETP 13 (1961) 451]
[6] Gross EP. Nuovo Cimento 1961;20:454.
[7] Gross EP. J Math Phys 1963;4:195.
[8] Johansson M, Hörnquist M, Riklund R. Phys Rev B 1995;52:231.
[9] Datta PK, Kundu K. Phys Rev B 1996;53:14929.
[10] Pan Z, Xiong S, Gong C. Phys Rev E 1997;56:4744.
[11] de Moura FAB, Gléria I, dos Santos IF, Lyra ML. Phys Rev Lett 2009;103:096401.
[12] Iomin A. Phys Rev E 2010;81:017601.
[13] Caetano RA, de Moura FABF, Lyra ML. Eur Phys J B 2011;80:321.
[14] Tietsche S, Pikovsky A. Europhys Lett 2008;84:10006.
[15] Dias WS, Lyra ML, de Moura FABF. Eur Phys J B 2012;85:7.
[16] Su WP, Schrieffer JR, Heeger AJ. Phys Rev Lett 1979;42:1698; Su WP, Schrieffer JR, Heeger AJ. Phys Rev B 1980;22:2099; Heeger AJ, Kivelson S, Schrieffer JR, Su W-P. Rev Mod Phys 1988;60:781.
[17] Dias WS, Lyra ML, de Moura FABF. Phys Rev B 2010;82:233102.
[18] de Moura FABF, Fulco UL, Lyra ML, Domnguez-Adame F, Albuquerque EL. Physica A 2011;390:535.
[19] Upadhyay PK, Nagar AK. Int J Mod Phys: Conf Series 2013;22:670.
[20] Filho VLC, Lima RPA, de Moura FABF, Lyra ML. Int J Mod Phys C 2015;26:1550133.
[21] de Moura FABF, Vidal EJGG, Gléria I, Lyra ML. Phys Lett A 2010;374:4152.
[22] Pikovsky AS, Shepelyansky DL. Phys Rev Lett 2008;100:094101.
[23] Mulanski M, Pikovsky AS. Eur Phys J B 2012;85:105.
[24] Lyra ML, Lima RPA. Phys Rev E 2012;85:057201.
[25] Silva AFG, Lima RPA, Chaves V, de Moura FABF, Lyra ML. Commun Nonlinear Sci Numer Simulat 2016;30:101.
[26] Neto AR, de Moura FABF. Commun Nonlinear Sci Numer Simulat 2016;40:6.
[27] Hairer E, Nørsett SP, Wanner G. Solving Ordinary Dierential Equations I: Nonstiff Problems. Berlin: Springr: Springer Series in Computational Mathematics; 2010; Press WH, Flannery BP, Teukolsky SA, Wetterling WT. Numerical Recipes: The Art of Scientific Computing 3rd edn. New York: Cambridge University Press; 2007.
[28] Kenkre VM, Wu H-L. Phys Rev B 1989;39:6907.
[29] Filho VLC, Lima RPA, Lyra ML. Chaos 2015;25:063101.